Modern Spectrum Sensing Techniques for Cognitive Radio Networks: Practical Implementation and Performance Evaluation

Antoni Ivanov, Nikolay Dandanov, Nicole Christoff, Vladimir Poulkov

Abstract—Spectrum underutilization has made cognitive radio a promising technology both for current and future telecommunications. This is due to the ability to exploit the unused spectrum in the bands dedicated to other wireless communication systems, and thus, increase their occupancy. The essential function, which allows the cognitive radio device to perceive the occupancy of the spectrum, is spectrum sensing. In this paper, the performance of modern adaptations of the four most widely used spectrum sensing techniques namely, energy detection (ED), cyclostationary feature detection (CSFD), matched filter (MF) and eigenvalues-based detection (EBD) is compared. The implementation has been accomplished through the PlutoSDR hardware platform and the GNU Radio software package in very low Signal-to-Noise Ratio (SNR) conditions. The optimal detection performance of the examined methods in a realistic implementation-oriented model is found for the common relevant parameters (number of observed samples, sensing time and required probability of false alarm).

Keywords—Cognitive radio, dynamic spectrum access, GNU Radio, spectrum sensing.

I. INTRODUCTION

IN the past decade, the number of applications which use Cognitive Radio (CR) has increased. The technology is being exploited to provide a method of using the spectrum more efficiently. That makes the area of spectrum sensing increasingly important and key to those applications. This requires that the overall system operates effectively and provides the required improvement in spectrum efficiency. The CR spectrum sensing system must be able to detect and identify any other transmissions and to inform the central processing unit within the CR so that the appropriate action can be taken.

The detection of Primary Users (PU) is performed based on the received signal at CR users. This approach includes methods, such as energy based detection [1], cyclostationary based detection [2], [3], matched filter based detection [4], eigenvalues-based detection [5], whose purpose is to detect the presence or absence of primary transmitter.

A. Ivanov is with the Faculty of Telecommunications, Technical University of Sofia, blvd. Kliment Ohridski 8, 1796 Sofia, Bulgaria (e-mail: astivanov@tu-sofia.bg).

N. Dandanov is with the Faculty of Telecommunications, Technical University of Sofia, blvd. Kliment Ohridski 8, 1796 Sofia, Bulgaria (e-mail: n_dandanov@tu-sofia.bg).

N. Christoff is with the Faculty of Telecommunications, Technical University of Sofia, blvd. Kliment Ohridski 8, 1796 Sofia, Bulgaria and Aix Marseille Univ, Université de Toulon, CNRS, LIS, France (e-mail : nicole.christoff@univ-amu.fr).

V. Poulkov is with the Faculty of Telecommunications, Technical University of Sofia, blvd. Kliment Ohridski 8, 1796 Sofia, Bulgaria (e-mail: vkp@tu-sofia.bg).

Kumar et al. [1] present some approaches for the energy detection technique and investigate the effect of different threshold selection methods on the spectrum sensing performance parameters. Banjade et al. [6] propose some approximations for performance of the energy detector, although offering computational ease, but not accurate for small sample sizes. In their work, Murty et al. [2] propose a cyclostationary based spectrum detection algorithm for Orthogonal-Frequency Division Multiplexing (OFDM) signals. The proposed architecture is hardware implemented in Field-Programmable Gate Array (FPGA) platform and its functionality and performance are verified with respect to conventional ones. Blad et al. [7] also consider spectrum sensing of OFDM signals and propose modifications to some state-of-the-art detectors, which are implemented using GNU Radio and USRP, and evaluated over a physical radio channel. Tani et al. focus on a low-complexity cyclostationary spectrum sensing of cognitive heterogeneous LTE-A network where the eNB represents the primary system. The third method, based on the matched filter technique, is characterized by a static sensing threshold. However, the noise is random, and [4] suggest a dynamic sensing threshold approach to increase the efficiency of the sensing detection. The eigenvalue-based method overcomes the highly vulnerable under noise uncertainty energy-based detection method, but but the performance deteriorates at low SNR. To solve this problem, the optimum number of samples, the theoretical analysis and numerical formula for given SNR are proposed in [5]. The optimal threshold minimizes the total error rate over a WGN channel and [8], based upon the optimal threshold theory, propose dynamic threshold scheme to reduce average total error rate for local CR node with applied energy detector.

The majority of spectrum sensing research works is performed theoretically and verified via computer simulations [9], [10]. Sardana and Vohra [10] evaluated the two important parameters for the channel sensing performance of energy detection, cyclostationary detection and matched filter. This analysis reports the detection probability and the false alarm probability. In [9], only the performance of energy detector and matched filter are compared, which is a common and well established practice. There have also been many practical realizations of CR systems [7], [11], [12] with a different range of scientific contributions but they are much fewer in comparison to the works which present solutions verified only via simulations.

The rest of the paper is organized as follows. Section

II describes the common description of the PU signal and noise used in all of the experiments in this study, and the models of the four detectors. Then, Section III introduces the hardware platform and the software used for the implementation. The setting and conditions of the experiments are explained in Section IV. Section V discusses the results of the measurements in terms of detection performance for the examined algorithms. Finally, the conclusions of this study are given in Section VI.

II. SYSTEM MODEL AND PRIMARY USER SIGNAL DETECTION

The premise which is described in this section will be applied for all detection algorithms examined in this study. It consists of a PU which has to be detected and a secondary user (SU) which needs to determine whether the PU's signal is present in the frequency band in question or not. They are both located in close proximity to one another as the scenario is relevant to indoor cellular networks or Internet of Things (IoT) system deployments. The signal of the PU is defined as an OFDM modulated data flow which is described as a Gaussian process and so is the noise. Due to the problem studied here, being detection of the PU signal, the input $y(k)$ of the receiver can be characterized in the following way:

$$y(k) = \begin{cases} n(k), & H_0 \\ s(k) + n(k), & H_1, \end{cases} \quad (1)$$

$n(k)$ representing the noise with zero mean and variance σ_n^2, and $s(k)$ - the signal of the PU with zero mean and variance σ_s^2. There are, thus, only two possibilities for the content of the information received by the detector - hypothesis H_0 which signifies that the PU is absent from the band, and H_1 where the signal is present and needs to be detected accurately despite of it being corrupted by noise and channel imperfections. It is required by each detection algorithm to identify the presence of the PU with a sufficient probability P_d while, at the same time, guaranteeing a desired probability of false alarm P_{fa} which describes the likelihood of the detector perceiving that the signal is present in the spectrum when in reality, it is not. The probability of detection secures the transmission of the PUs from harmful interference while a low probability of false alarm provides the SU with the opportunity of higher utilization of the available spectrum. These are the general concepts of the scenario in which all four detector types will be examined.

A. Energy Detection

This technique has been the object of great many scientific studies for many years and especially since the rise of the CR concepts in the last two decades. This is due to it being the simplest to implement and most computationally effective [13]. In addition to this, the ED allows an almost blind detection algorithm which can be applied to all kinds of signals. Its major drawback is its unreliability in below-zero SNR conditions due to it being unable to discriminate between different kinds of signals. For that reason it is necessary to

precisely determine the noise level and the decision threshold which can be difficult in realistic implementations. For this study, the energy-based spectrum sensing method explored in [1], [14] is chosen due to its promising adaptive threshold feature. The test statistic of the signal, which is compared against the threshold to determine the occupancy of the spectrum, is defined as follows:

$$T(y) = \frac{1}{N} \sum_{k=0}^{N-1} y(k), \quad (2)$$

where N is the number of received samples by the detector. Then the threshold λ is defined as [1]:

$$\lambda = \frac{-B - \sqrt{B^2 - 4AC}}{2A},$$
$$A = \frac{-B}{2N} \left(\frac{1}{\sigma_t^2} + \frac{1}{\sigma_n^2} \right), \quad (3)$$

$$B = \frac{\sigma_s^2}{\sigma_t^2 \sigma_n^2}; \ C = \frac{-2 \log \left(\frac{\sigma_n^2}{\sigma_t^2} \right)}{\log(e)}; \ \sigma_t^2 = \sigma_n^2 + \sigma_s^2.$$

The performance of the detector is determined through the widely-used equation for P_d [14], [15] which is applicable due to the PU signal and noise following a Gaussian distribution and the number of samples being more than a few hundred [1], [14], [15].

B. Cyclostationary Detection

This type of detector extends the capabilities of the spectrum sensing function by allowing better detection in low SNR and fading for much lower number of samples than the energy detection [3], [11], [12]. The algorithm utilizes the presence of characteristic cyclostationary features in the communications signals. Noise is differentiated from the PU signal by examining whether the test statistic includes these features or not. Their main advantage is that they remain present even if the noise level is much higher than that of the signal. The test statistic $T(y)$ chosen for the following comparison uses the Cyclic Autocorrelation Function (CAF) of the Single Cycle Detector with Sliding Correlation (SCD-SC) proposed in [3] due to its decreased computational complexity:

$$T(y) = \left| \hat{R}_y^\alpha (\tau) \right|^2$$

$$\hat{R}_y^\alpha (\tau) = \frac{1}{N} \frac{1}{M} \sum_{k=0}^{N-1} \sum_{i=k}^{n+M-1} y(i) y^*(i+\tau) e^{-j2\pi\alpha k}, \quad (4)$$

where $\hat{R}_y^\alpha$ is the CAF of the received signal y which is examined for the two features of the PU signal – the cyclic frequency α and time lag τ [16]. N is the number of observed samples and M is the quantity of samples which are contained in the sliding window. The decision threshold for this cyclostationary detector is [3]:

$$\lambda = -\frac{2\sigma_n^4 \ln (P_{fa})}{NM}. \quad (5)$$

Similarly to [3], [12], the Rayleigh fading scenario is considered which leads to the following expression for the

P_d [3]:

$$P_d = \int_{min(h)}^{max(h)} Q_1\left(\frac{\gamma_f}{\nu_f}, \frac{\sqrt{\lambda}}{\nu_f}\right) \frac{e^{\frac{-h^2}{\mu}}}{\mu}\, dh^2,$$

$$\nu_f = \frac{\sigma_n^2 + \sigma_s^2 h^2}{\sqrt{NM}};\ \gamma_f = \left|\hat{R}_y^\alpha\right| h^2. \tag{6}$$

The integral is defined within the lowest and highest values of the channel estimation vector h and μ is the mean of its distribution, $Q_1(.)$ being the Marcum Q function of first order [17] which can be computed using the algorithm proposed in [18].

C. Eigenvalue-Based Detection

In this case, further accuracy and robustness to noise is sought by exploring a more complex mathematical derivation of the test statistic [5]. It is expressed by the ratio of the maximum γ_{max} and minimum γ_{min} eigenvalue of the covariance matrix $\boldsymbol{R}_r$ formed by performing the following operations. First, the vector of N received samples is split into L (L is the smoothing factor) equal parts and a matrix $\boldsymbol{Y}$ with shape $L \times N_L$ is formed, where $N_L = \frac{N}{L}$. Finally $\boldsymbol{R}_r$ is obtained [11]:

$$\boldsymbol{R}_r = \frac{1}{N_L}\boldsymbol{Y}\boldsymbol{Y}^*. \tag{7}$$

The threshold λ is defined as [5], [11]:

$$\lambda = \frac{\chi^2}{\delta^2}\left(1 + \frac{\chi^{-2/3}}{(NN_L^2)^{1/6}} F_2^{-1}(1 - P_{fa})\right), \tag{8}$$

where $\chi = \left(\sqrt{N_L} + \sqrt{NN_L}\right)$, $\delta = \left(\sqrt{N_L} - \sqrt{NN_L}\right)$ and $F_2^{-1}(.)$ is the inverse Tracy-Widom distribution of second order [19] which is used in the case of complex samples as it is in this study. To determine the performance of the EBD, the expression for P_d derived in [5] is used:

$$P_d = 1 - F_2\left(\kappa\right), \tag{9}$$

where

$$\kappa = \frac{\frac{N_L}{\sigma_n^2}\left(\lambda\gamma_{min}(\boldsymbol{R}_n(N_L)) + \lambda\rho_{min} - \rho_{max}\right) - \psi}{\phi}$$

$$\psi = (\sqrt{N_L - 1} + \sqrt{L})^2,$$

$$\phi = (\sqrt{N_L - 1} + \sqrt{L})\left(\frac{1}{\sqrt{N_L - 1}} + \frac{1}{L}\right)^{1/3}.$$

The parameters $\gamma_{min}(\boldsymbol{R}_n(N_L))$, ρ_{min} and ρ_{max} are the minimum eigenvalue of the covariance matrix of the noise, the minimum and maximum eigenvalues of the covariance matrix of the PU signal. They are all computed in the same way as the covariance matrix of the received samples and its eigenvalues (γ_{max} and γ_{min}). $F_2(.)$ is the Tracy-Widom distribution of second order which is calculated using tabular data found in [20]. As taken from [5], L is set to 5.

D. Matched Filter Detection

The detector based on the MF is characterized by achieving optimal performance in case the probability density function (PDF) of the PU signal is known (as it is in the present study) [21]. That is due to the use of specific information about the signal which needs to be identified. This is the main disadvantage of the MF. The information is usually in the form of the pilot signal x_p. Thus, the test statistic and the decision threshold have the form [4], [21]:

$$T(y) = \sum_{k=0}^{N-1} y(k)x_p^*(k)$$

$$\lambda = Q^{-1}(P_{fa})\sqrt{E\sigma_n^2}, \tag{10}$$

where E is the energy of the PU pilot signal and $Q^{-1}(.)$ is the inverse Q-function defined as $Q^{-1}(u) = \sqrt{2}\,\mathrm{erfc}^{-1}(2u)$, erfc^{-1} being the inverse complimentary error function. The probability of detection which characterizes the efficiency of the algorithm is [4], [21]:

$$P_d = Q\left(\frac{\lambda - E}{\sqrt{E\sigma_n^2}}\right), \tag{11}$$

where $Q(.)$ is the Q-function which is expressed as $Q(u) = \frac{1}{\sqrt{2\pi}}\int_u^\infty exp\left(-\frac{v^2}{2}\right) dv$.

III. Measurement Equipment and Software

For the purpose of our experiment, the GNU Radio software development toolkit and two ADALM-PLUTO Software-Defined Radios (SDRs) were used. GNU Radio provides signal processing blocks to implement SDR and also contains the Companion, a graphical user interface similar to Simulink for creating signal flow graphs and generating flow-graph source code [22]. In our scenario, various blocks provided by GNU Radio are directly utilized in our Python source code without using the Companion.

The ADALM-PLUTO Active Learning Module (PlutoSDR) is based on Analog Devices AD9363, a Radio Frequency (RF) 2×2 transceiver with integrated 12-bit Digital-to-Analog Converters (DACs) and Analog-to-Digital Converters (ADCs), and on Xilinx Zynq Z-7010 FPGA. The SDR offers one receive channel and one transmit channel which can be operated in full duplex, capable of generating or measuring RF analog signals from 325 to 3800 MHz, at up to 61.44 Mega Samples per second (MS/s) with a 20 MHz bandwidth. The transmit power output is up to 7 dBm and the receive Noise Figure is rated at < 3.5 dB. The PlutoSDR is widely supported under various software suites, including GNU Radio, MATLAB, Simulink, libiio, and offers Application Programming Interfaces (APIs) for C, C++, C#, and Python [23].

In our setup, each of the PlutoSDR units was connected to a host computer using the USB 2.0 interface and communicated via Ethernet over USB, through which complex I/Q samples were carried. The host computers for the transmitter and receiver units were running 64-bit Linux operating systems – Debian Stretch and Ubuntu Xenial, respectively. The PlutoSDR units run embedded Linux. The two units we used are depicted in Fig. 1.

Fig. 1 A photograph of the PlutoSDR units used for our experiments

Fig. 2 A photograph of the PlutoSDR units during the measurements

IV. Experimental Setting and Implementation Details

The experiment was conducted in an indoor environment (in the premise of a room, see Fig. 2) using two PlutoSDRs, one being the transmitter (Tx) and the other - the receiver (Rx) which implements the detectors. In this way, a realistic scenario is represented due to the non-line-of-sight (NLOS) conditions and Rayleigh fading. Transmission is implemented by building a GNU Radio graph which includes the OFDM Modulator block from the *gr-digital* GNU Radio package, to form the PU signal. To emulate a realistic transmitter, the executed flow of the graph is controlled through the Python file which GNU Radio generates. In this way, discontinuous transmission is implemented by setting an array of busy and idle (ON and OFF) time periods for the transmitter. These periods follow a Generalized Pareto distribution because it has been shown to be the most accurate model for modern cellular systems [24]. The two parameters which define the distribution are $\{1.3692, -0.2669\}$ for the busy periods and $\{10.3225, 0.4805\}$ for the idle and are obtained from [24]. The samples drawn from these distributions are the values of the arrays of busy and idle periods of the transmitter. Thus, discontinuous transmission is run in the span of 5 minutes during which the receiver is performing the detection.

The SU receiver is implemented by utilizing a GNU Radio flow-graph which obtains the signal samples and processes them using the Fast Fourier Transform (FFT) block with size 1024 and then outputs them into the *Message Sink* block which allows for the actual detection to be performed in real time inside the Python script. For each of the detectors, the program runs for 5 minutes during which it collects samples for 0.5 seconds and then calculates the decision threshold, the test statistic and determines whether the PU is present in the spectrum. Due to the limitations of the currently used PLUTO SDR model (Fig. 1), the minimum supported bandwidth of 600 kHz is used. Such consideration is due to this model providing only USB 2.0 functionality for transfer to the host computer. Another limitation of the transceiver is the frequency range which is the reason the experiment was conducted in an available Wireless Local Area Network (WLAN) channel in the 2.4 GHz industrial, scientific and medical (ISM) spectrum band. The receiver gain is 40 dB while the attenuation of the transmitter is 20 dB which makes the output power to be -13 dBm. As a logical consequence of the bandwidth being 600 kHz, the sampling rate F_s is 1.2 MS/s. Therefore, at each iteration of the measurements, there are about 300 000 complex samples provided to the SDR for the sensing time of 500 ms. Several considerations are made in regards to the implementation of the detectors in a practical experiment. First of all, the SNR level is estimated using the full-scale SNR method described in [7]. The sensing time during which the measurements are performed is set to 1.5 seconds due to the CR standard [25] allowing up to 2 seconds for the detection to be executed. Requirements set by the standard also give the desired constant P_{fa} to be 0.1. The noise power and variance are estimated using 1 million samples when the transmitter is in idle state. Likewise, the reference power and variance of the PU signal is computed by measuring 1 million samples under the condition that the transmitter is 1 meter away from the receiver. That is also used to estimate the reference for the full-scale SNR. This PU signal vector is used instead of a pilot signal in the case of the MF detector because the actual transmitted data remains always the same in this experiment. This is due to the fact that the contents of the PU signal are irrelevant because it is generalized. For the CSFD, the implementation considerations in [12] are made. Thus, the features of the OFDM signal are $\alpha = 0.2F_s = 240$ kHz and $\tau = 256$ samples. The estimation of the channel vector for the calculation of the integral in (6) also follows the algorithm described in [12]. Due to the complexity of this algorithm being much greater than that of the other three, the number of samples utilized for it are limited to 3000. That is necessary in order for the processing to be performed in a reasonable amount of time.

V. Measurement Results

This section will present the analysis of the measurement results in the previously described environment and system model. The performance results for the four detectors are presented in 3.

It is easily observed that in the current setting, the optimality of the MF-based detector is proven. This distinction holds
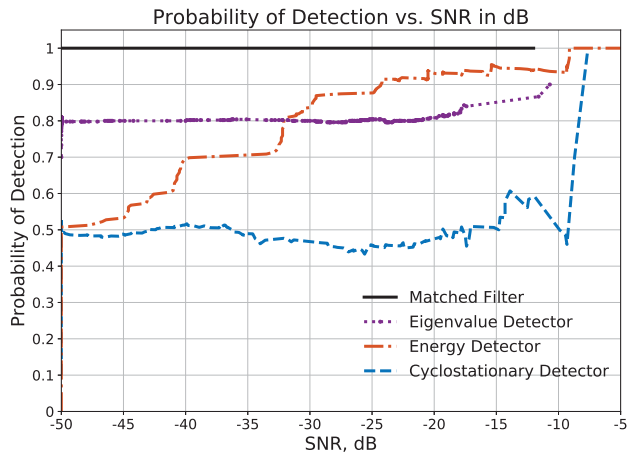
Fig. 3 Probability of detection versus the measured SNR for the four detectors

due to the definition of the PU OFDM signal model which allows for generalization and does not require demodulation and feature extraction from a pilot signal. The paper [4] which describes the model further solidifies this observation because it shows that for high number of samples (as it is in this case), the detector reaches excellent performance. When it comes to the CSFD, it is evident that despite of it operating in very limited number of samples as stated in the previous section, has achieved fair efficiency even though it is worse compared to the other three detectors. The ED has shown significant performance surpassing the CSFD and EBD for SNR over -30 dB. This can be attributed to the large number of samples which naturally increase the P_d. Finally, the EBD statistic shows that the computation of the eigenvalues of the covariance matrix allow high discrimination of the signal from the noise even in very low SNR levels. It is however, unable to reach optimal detection in this setting. It is evident that all detectors achieve at least 50 % efficiency at even -50 dB which is due to their characteristics and the large number of samples obtained by the receiver for the chosen sensing period (500 ms).

VI. CONCLUSION

This paper has presented a study of the implementation and comparison of the effectiveness of four contemporary detection algorithms. The details of the experimental procedures have also been described. Out of the four detectors, only ED and MF achieved the performance of 90% probability of detection at SNR of -20 dB, required in the CR standard [25]. This underlines the necessity of algorithms which allow simple signal processing which allows for more samples to be observed. Due to the non-uniformity of areas where the signal detectors need to be applied within IoT, any of the examined types of detectors can be utilized depending on what information about the PU signal is known at the SU device, and how much computational power this device possesses. The examination conducted reveals their agility and potency for practical experimentation.

REFERENCES

[1] A. Kumar, P. Thakur, S. Pandit, and G. Singh, "Performance analysis of different threshold selection schemes in energy detection for cognitive radio communication systems," in *Image Information Processing (ICIIP), 2017 Fourth International Conference on*. IEEE, 2017, pp. 1–6.

[2] M. S. Murty and R. Shrestha, "VLSI architecture for cyclostationary feature detection based spectrum sensing for cognitive-radio wireless networks and its asic implementation," in *VLSI (ISVLSI), 2016 IEEE Computer Society Annual Symposium on*. IEEE, 2016, pp. 69–74.

[3] A. Tani, R. Fantacci, and D. Marabissi, "A low-complexity cyclostationary spectrum sensing for interference avoidance in femtocell LTE-A-based networks," *IEEE Transactions on Vehicular Technology*, vol. 65, no. 4, pp. 2747–2753, 2016.

[4] F. Salahdine, H. El Ghazi, N. Kaabouch, and W. F. Fihri, "Matched filter detection with dynamic threshold for cognitive radio networks," in *Wireless Networks and Mobile Communications (WINCOM), 2015 International Conference on*. IEEE, 2015, pp. 1–6.

[5] C. Charan and R. Pandey, "Eigenvalue-based reliable spectrum sensing scheme for cognitive radio networks," in *Nascent Technologies in Engineering (ICNTE), 2017 International Conference on*. IEEE, 2017, pp. 1–5.

[6] V. R. S. Banjade, C. Tellambura, and H. Jiang, "Approximations for Performance of Energy Detector and p-Norm Detector," *IEEE Communications Letters*, vol. 19, no. 10, pp. 1678–1681, 2015.

[7] A. Blad, E. Axell, and E. G. Larsson, "Spectrum sensing of OFDM signals in the presence of CFO: New algorithms and empirical evaluation using USRP," in *Signal Processing Advances in Wireless Communications (SPAWC), 2012 IEEE 13th International Workshop on*. IEEE, 2012, pp. 159–163.

[8] X. Zhai, H. Haigen, and Z. Guoxin, "Optimal threshold and weighted cooperative data combining rule in cognitive radio network," in *Communication Technology (ICCT), 2010 12th IEEE International Conference on*. IEEE, 2010, pp. 1464–1467.

[9] A. F. Eduardo and R. G. G. Caballero, "Experimental evaluation of performance for spectrum sensing: Matched filter vs energy detector," in *Communications and Computing (COLCOM), 2015 IEEE Colombian Conference on*. IEEE, 2015, pp. 1–6.

[10] M. Sardana and A. Vohra, "Analysis of different spectrum sensing techniques," in *Computer, Communications and Electronics (Comptelix), 2017 International Conference on*. IEEE, 2017, pp. 422–425.

[11] A. Nafkha, B. Aziz, M. Naoues, and A. Kliks, "Cyclostationarity-based versus eigenvalues-based algorithms for spectrum sensing in cognitive radio systems: Experimental evaluation using GNU radio and USRP," in *Wireless and Mobile Computing, Networking and Communications (WiMob), 2015 IEEE 11th International Conference on*. IEEE, 2015, pp. 310–315.

[12] A. Ivanov, A. Mihovska, K. Tonchev, and V. Poulkov, "Real-time adaptive spectrum sensing for cyclostationary and energy detectors," *IEEE Aerospace and Electronic Systems Magazine*, vol. 33, no. 5-6, pp. 20–33, 2018.

[13] B. Wang and K. R. Liu, "Advances in cognitive radio networks: A survey," *IEEE Journal of selected topics in signal processing*, vol. 5, no. 1, pp. 5–23, 2011.

[14] X. Zhai, H. Haigen, and Z. Guoxin, "Optimal threshold and weighted cooperative data combining rule in cognitive radio network," in *Communication Technology (ICCT), 2010 12th IEEE International Conference on*. IEEE, 2010, pp. 1464–1467.

[15] H. Urkowitz, "Energy detection of unknown deterministic signals," *Proceedings of the IEEE*, vol. 55, no. 4, pp. 523–531, 1967.

[16] W. A. Gardner and C. M. Spooner, "Signal interception: performance advantages of cyclic-feature detectors," *IEEE Transactions on Communications*, vol. 40, no. 1, pp. 149–159, 1992.

[17] S. András, A. Baricz, and Y. Sun, "The generalized marcum q-function: an orthogonal polynomial approach," *Acta Universitatis Sapientiae Mathematica*, vol. 3, no. 1, pp. 60–76, 2011.

[18] W. McGee, "Another recursive method of computing the q function (corresp.)," *IEEE Transactions on Information Theory*, vol. 16, no. 4, pp. 500–501, 1970.

[19] C. A. Tracy and H. Widom, "On orthogonal and symplectic matrix ensembles," *Communications in Mathematical Physics*, vol. 177, no. 3, pp. 727–754, 1996.

[20] A. Bejan, "Largest eigenvalues and sample covariance matrices. tracy-widom and painleve ii: computational aspects and realization in s-plus with applications," *Preprint: http://www. vitrum. md/andrew/MScWrwck/TWinSplus. pdf*, 2005.

[21] S. M. Kay, "Fundamals of statistical signal processing. detection theory, volume ii," 1998.

[22] The GNU Radio Foundation, "GNU Radio, the free and open software radio ecosystem," http://gnuradio.org, [Online]. Accessed: 28. June 2018.

[23] Analog Devices, Inc., "ADALM-PLUTO — Software-Defined Radio Active Learning Module," http://www.analog.com/en/design-center/ evaluation-hardware-and-software/evaluation-boards-kits/adalm-pluto. html, [Online]. Accessed: 28. June 2018.

[24] M. López-Benítez and F. Casadevall, "Time-dimension models of spectrum usage for the analysis, design, and simulation of cognitive radio networks," *IEEE transactions on vehicular technology*, vol. 62, no. 5, pp. 2091–2104, 2013.

[25] C. R. Stevenson, G. Chouinard, Z. Lei, W. Hu, S. J. Shellhammer, and W. Caldwell, "Ieee 802.22: The first cognitive radio wireless regional area network standard," *IEEE communications magazine*, vol. 47, no. 1, pp. 130–138, 2009.